JOURNAL OF MATERIALS SCIENCE 28 (1993) 3547–3556

Synthesis of cubic boron nitride using Mg and pure or M′-doped Li_3N, Ca_3N_2 and Mg_3N_2 with M′=Al, B, Si, Ti

G. BOCQUILLON, C. LORIERS-SUSSE, J. LORIERS
Laboratoire de Physicochimie des Matériaux, CNRS, 1 Place Aristide Briand, 92195 Meudon Principal Cedex, France

The growth pressure–temperature region of cubic boron nitride (cBN) in the systems Mg–BN and MxNy–BN (MxNy = Li_3N, Ca_3N_2, Mg_3N_2) has been redetermined using well-crystallized hexagonal BN (hBN) with low oxygen content (0.2%) as the starting material. The data on the MxNy–BN systems are compatible with the existence of two growth regions: a high-temperature region where cBN grows from a liquid phase, and a low-temperature region where cBN forms from solid–solid reactions. Previous data are discussed according to this model and possible solid-state reactions are proposed on the basis of thermodynamic considerations. The results for the Mg–BN system confirm the effect of the O_2 content of the starting BN on the cBN growth region. The systems (MxNy + M′)–BN (M′ = Al, B, Si, Ti) have been shown to produce cBN crystals of increased size and improved morphology (more compact and perfect) compared to those obtained with the MxNy–BN systems. Their colour is dark or black and their size reaches 0.6 mm. The effect of the relative proportions of M′ and MxNy on the growth region and yield has been determined and is discussed on the basis of the chemical reactions likely to occur.

1. Introduction

Cubic boron nitride (cBN) is a synthetic product which has important applications as a superhard material. Second only to diamond in its hardness, its high thermostability and low chemical reactivity with transition-metal alloys make it an unequalled substitute to diamond for the machining of ferrous materials. cBN single crystals larger than 10 μm are generally obtained by a nucleation and growth process in which hexagonal boron nitride (hBN) is dissolved in a flux at high pressure [1]; cBN crystallizes from this flux when the pressure and temperature (P–T) conditions fall into its thermodynamic stability field. If alkali or alkaline-earth nitrides are used as initiators of the synthesis, high yields are attained especially with Li_3N, Ca_3N_2 and Mg_3N_2. Then the fluxes consist of the boronitrides Li_3BN_2 [2], $Ca_3B_2N_4$ [3] and $Mg_3B_2N_4$ [4] formed by reaction of the nitrides with BN. The cBN crystals obtained are of the orange–yellow variety and their size rarely surpasses 0.25 mm: a limit set by the difficulties encountered in controlling the nucleation. When alkali or alkaline-earth metals are used instead of their nitrides, however, the fluxes differ in that they contain boron in excess from the composition of the boronitrides. This results in the brown or black colour exhibited by cBN crystals which contain excess boron [1]. The crystals are occasionally of a larger size and adopt more compact shapes; however, their yield is low, probably as a consequence of the lower reactivity of the metals with BN compared to that of the nitrides.

Because of the increased compactness of the crystals, which favours high mechanical resistance, and of their increased size, it seemed interesting to look for systems leading to fluxes of composition similar to that realized with the alkali or alkaline-earth metals while using initiators more reactive than these to increase the yield. During this search it was found that addition to the nitrides mentioned above, M_xN_y, of an element, M′, able to reduce them could fulfil the purpose. It is believed that the reduction gives rise to activated species which are more reactive than the metals in the atomic state. Al, B, Si and Ti were found to be suitable elements to use (as M′) in addition to Li_3N, Ca_3N_2 and Mg_3N_2. Ordered hBN was used throughout the work as a starting material. In most cases compact crystals of improved morphology, compared to those obtained with the pure nitrides, were synthesized. Their size reached 0.60 mm and the yield was comparable to that observed with the nitrides.

The results are interpreted on the basis of data known for the M–M′–N systems at ambient pressure.

2. Experimental procedure

The experiments were performed in an apparatus of

0022–2461

the belt type using the cell arrangement shown in Fig. 1. To protect the reactive mixture against pollution, dehydroxylated pyrophyllite or an MgO-based machinable ceramic (Alsimag 222, General Electric Ceramics) was used to contain the graphite heater. The pressure was deduced from the applied force using a preliminary calibration at 20 °C based on the phase transformations of bismuth at 2.54 and 7.7 GPa and of thallium and barium at 3.68 and 5.5 GPa, respectively. This was corrected to include the heating effect on pressure from the growth P–T conditions of diamond in the Co–C system [5, 6]. The temperature was obtained from power–temperature curves established using Pt/Pt 10%Rh thermocouples after correction of the pressure effect on the electromotive force (e.m.f.) [7]. In the experiments, pressure and temperature were simultaneously increased to the maximum values and maintained there for 3 min. The power was then turned off and the pressure was decreased to zero.

The reactive mixture recovered was treated chemically and physically to isolate the cBN formed. HCl or water, depending on the initiator, was used to dissolve the flux and a fluorating mixture (H_2SO_4 + NaF) was used to dissolve the remaining hBN and the silicates coming from the surrounding medium. A separation by flotation in bromoform completed the operation. The cBN crystals were examined using optical microscopy, scanning electron microscopy (SEM) and X-ray diffraction (XRD).

2.1. Starting products

2.1.1. hBN

The main characteristics of the products used in this study are given in Table I. Well-crystallized hBN was used in all runs. The graphitization index, *I*, as defined by Thomas *et al.* [8] was determined from X-ray diffractograms. In agreement with previous findings, the grain size and purity of hBN had an important effect on the yield. Grade A hBN from Carborundum containing 4–6% O_2 was found unsuitable because of its low cBN yield and was only used in a preliminary study of the Mg–BN system. Among the sintered products, the HP grade hBN from Carborundum and ASBN grade hBN from ESK (Germany) gave good results and were indifferently used for part 1 of the cell (Fig. 1). A net increase in the yield was observed when parts 2 were made of pressed pellets of powder instead of sintered BN, an effect which may partly come from the lower oxygen content of the powders in addition to their higher reactivity. Among these, the very fine GREPSI (France) and ESK powders gave higher yields than the coarser ones. However, they were not used because it was not possible to get dense compacts by pressing them in air. Indeed a reproducible high density of the pellets is necessary to compare the yields and synthesis pressures in the different systems. Moreover, less dense pellets would lead to an important pressure loss in apparatus of larger volume, where the ratio of sample volume to cell volume is high. Therefore HTP-grade powder from Carborundum pressed to 0.5 GPa in a steel die was used in all runs. The density of the pellets was 1.93×10^3 kg m^{-3} (85% of the theoretical value).

Both sintered and powder parts were heated to 400 °C under vacuum for 12 h, so they were dehydrated before the runs.

2.1.2. Nitrides

Commercial nitrides of stated purity 94%, 98% and 99% for Li_3N, Ca_3N_2 and Mg_3N_2, respectively, were used. XRD for Li_3N revealed the presence of lithium in the product. This is taken into account in the discussion below. These three compounds, which are hygroscopic, were kept in a glove box where the operations of grinding, weighing, mixing and precompaction by hand in a steel die were made. In the case of Ca_3N_2, the most hygroscopic, compaction to the final pressure was also made in the glove box.

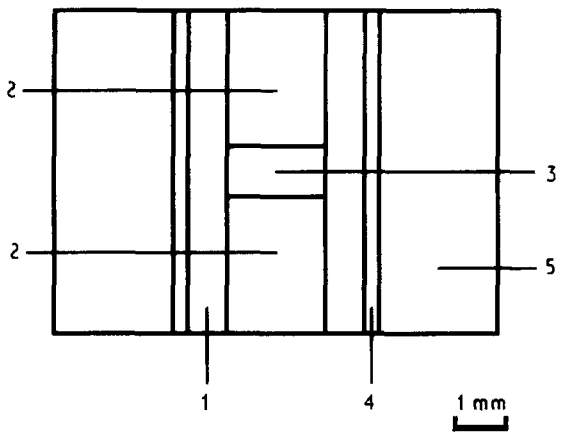

Figure 1 High pressure cell: (1) and (2) hBN, (3) initiator, (4) graphite, and (5) fired pyrophyllite or alsimag 222.

TABLE I Characteristics of the starting BN

Origin	Grade	(%)O	Form	Particle size (μm)	Graphitization index, *I*	Compaction	cBN yield
Carborundum	A	4–6	Sintered				*
Carborundum	HP	1.5–2.5	Sintered				**
ESK	ASBN	1	Sintered				**
Carborundum	HTP	0.2	Powder	< 40	2.08	Good	***
GREPSI		1.5	Powder	< 5	1.71	Bad	****
ESK	S, SX	1.5	Powder	0.5–1		Bad	****

2.1.3. M′ elements

The grain size and purity of Al, B, Si, Ti are given in Table II. They were stocked and handled in a glove box.

TABLE II Characteristics of M′ metal powders

	Element				
	B	Al	Ti	Si	Mg
Purity (%)	98	99.5	99.9	99.95	99.8
Particle size (μm)	50	50	60	40	50

3. Results and discussion

As a basis for comparison between the results with pure and doped nitrides, the P–T formation diagrams of cBN were redetermined, with Li_3N, Ca_3N_2 and Mg_3N_2 as initiators. This was necessitated by the marked differences, established by previous authors, between the diagrams. For the synthesis with doped nitrides (MxNy′ + M′), extended P–T diagrams were not determined, rather, a P–T region was chosen for study where convenient values of the yield and crystal size could be obtained. This region extended from 1600–1850 °C and 5–6.5 GPa.

The position of the hBN–cBN equilibrium boundary is not precisely known; in Figs 2, 4, 6, 7, two lines have been drawn, the Bundy–Wentorf [9] equilibrium line corrected for the new high-pressure scale by Tani *et al.* [10] and the line proposed by Rapoport [11] to take account of the experiments of Corrigan and Bundy [12]. The experimental high-temperature boundaries of the cBN formation diagrams suffer from large uncertainties and the discrepancies between different authors are believed to arise mainly from such factors as different thermal effects on pressure (which may differ in sign) because of the apparatus, different effects of pressure on the e.m.f. of thermocouples, and extrapolation of power versus temperature curves.

The results concerning pure initiators will be discussed first.

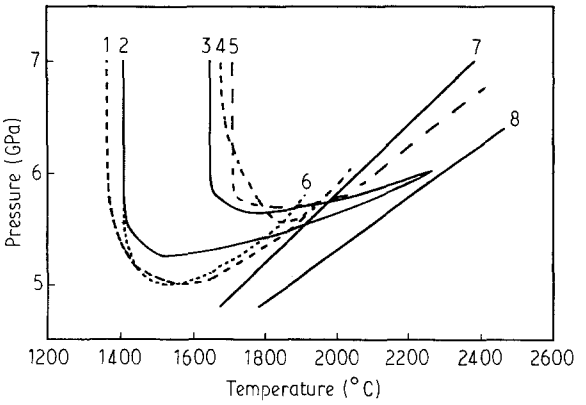

Figure 2 Cubic BN growth region in the Mg–BN system. Cubic BN exists in the region above each curve. The O_2% in the starting hBN is indicated in parentheses. (1) Endo *et al.* (2%) [13], (2) this work (0.2%), (3) this work (4%), (4) Endo *et al.* (8%) [13], (5) Kudaka *et al.* [16], (6) Bindal *et al.* (9%) [15], (7) Bundy–Wentorf hBN–cBN equilibrium line (see text), (8) close-to-true hBN–cBN equilibrium line after Rapoport (see text). For clarity, the data of Fukunaga *et al.* (4% O_2) [14], which lie very close to curve 5 are not shown.

3.1. M–BN and MxNy–BN systems

3.1.1. Mg–BN

3.1.1.1. P–T diagram. The results of the present work and of previous research on cBN formation in this system are summarized in Fig. 2. They prompt the following remarks. Firstly Endo *et al.* [13] and the authors observed that the oxygen content (indicated in the figure caption) of the starting BN affected the minimum temperature of cBN synthesis while Fukunaga *et al.* [14] and Bindal *et al.* [15] question this effect. Oxygen present as B_2O_3 in BN reacts with Mg_3N_2 according to the reaction

$$B_2O_3 + Mg_3N_2 \rightarrow 3MgO + 2BN$$

Information on the oxygen content in the work of Kudaka *et al.* [16] and Ushio [17] is lacking, although the presence of MgO in the reacted products of the former authors is evident on the X-ray powder patterns. The data of Ushio *et al.* [17] will not be discussed here because of their probable large temperature uncertainties due to their use of a platinum heater. The remaining data fall into two groups according to the minimum synthesis temperature which lies around 1380 or 1680 °C. Our results with BN containing 2 and 5% O_2 confirm the splitting of the low-temperature boundary observed by Endo *et al.* [13] with 2 and 8% O_2. However the data of Bindal *et al.* [15] with 9% O_2 content fall close to the 2% O_2 group and led their author to question the effect of the oxygen content on the yield and formation diagram of cBN [18]. An explanation of this discrepancy may lie in the cell arrangement used by Bindal [15] and his coworkers as the reactants Mg and hBN were intimately mixed powders in contrast to the alternately piled disks (see Fig. 1) used by the other workers. In the first case, a large number of nuclei rapidly form at the extended interface between the powders before the screening effect of MgO appears. In the second case, the MgO formed during the reaction accumulates at the interface, cBN–$Mg_3B_2N_4$ and hinders further nucleation and growth of cBN.

If the low-temperature boundaries of Fig. 2 are compared with those of the Mg_3N_2–BN shown in Fig. 7, the low-oxygen-content boundary is seen to coincide approximately with the temperature-of-first-appearance of a liquid phase (1380 °C) associated with eutectic melting (see Mg_3N_2–BN system, Section 3.1.4.). This shows that the by-products formed in the reaction of Mg and with BN (see Filonenko *et al.* [19]), other than $Mg_3B_2N_4$, leave this temperature grossly unaltered. Moreover no such boundary showing a negative slope, as in the Mg_3N_2–BN system is present in Fig. 2, perhaps because of a lower reactivity of Mg with BN compared to its nitride. All previous data for the high-temperature boundaries of Fig. 2 lie close to the Bundy–Wentorf equilibrium line. Our results show a distinct slope, and they approach the

close-to-true line proposed by Rapoport. As mentioned earlier, this difference is probably due to temperature affecting pressure calibration, which was considered only in our work.

3.1.1.2. cBN crystals. Black or dark brown octahedral crystals up to 0.15 mm were obtained (Fig. 3) at the higher temperatures and smaller (up to 0.05 mm) yellow, opaque, tetrahedral crystals, most often agglomerated, at the lower temperatures. The yield was much lower than with any of the other nitrides studied.

3.1.2. Li_3N–BN

3.1.2.1. P–T diagram. The formation diagrams of cBN from this system (reported in the literature and obtained in this work) are shown in Fig. 4. Compared to the other data, the data obtained by Vereshchagin *et al.* [20] show large differences which cannot be discussed due to lack of information on the experiments.

The data of De Vries and Fleisher [2] and Fukunaga *et al.* [14] are in good agreement with each other except that the minimum synthesis pressure is given as 4.8 or 5.3 GPa, respectively, and except that the diagrams show high-temperature boundaries which lie about 0.3 GPa higher than the Bundy–Wentorf equilibrium line. The present work gives a minimum pressure of 5 GPa and a high-temperature boundary approaching the equilibrium line proposed by Rapport. This different behaviour is probably due to the pressure calibration of our apparatus which was made at high temperature contrary to the other authors, as already mentioned in connection with the Mg–BN system.

The minimum synthesis temperature found by De Vries and Fleisher [2] and Fukunaga *et al.* [14] about 1600 °C at 6 GPa, is in agreement with the eutectic melting temperature in the Li_3N–BN system determined by De Vries and Fleisher. The minimum synthesis temperature found in the present work is about 200 °C lower than in the cited works; this discrepancy certainly exceeds the error limits, and can be explained as follows. It was observed that the low-temperature zone of the graph can be divided into two parts corresponding to a different morphology and yield of the cBN crystals and separated by a vertical line (shown as line 3 in Fig. 4) at approximately 1530 °C. At $T > 1530$ °C, euhedral crystals grow with facets indicating growth from a liquid phase and the yield is large. This temperature threshold is close to the minimum synthesis temperature (approximately 1550 °C) observed by Kudaka *et al.* [16] in the system Li–BN, and by De Vries and Fleisher [2] in the Li_3N–BN–B–Li portion of the Li–B–N system. Thus it seems that in our experiments the small amount of Li present in the starting Li_3N (see above) – perhaps increased by some decomposition of this compound by a reaction with the graphite heater which liberated Li – decreased the temperature-of-appearance of the liquid phase by about 80 °C. A large decomposition is

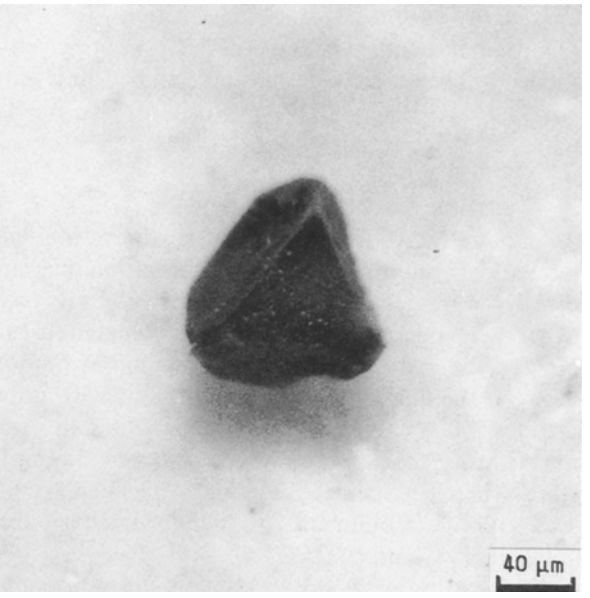

Figure 3 Cubic BN crystal grown in the Mg–BN system.

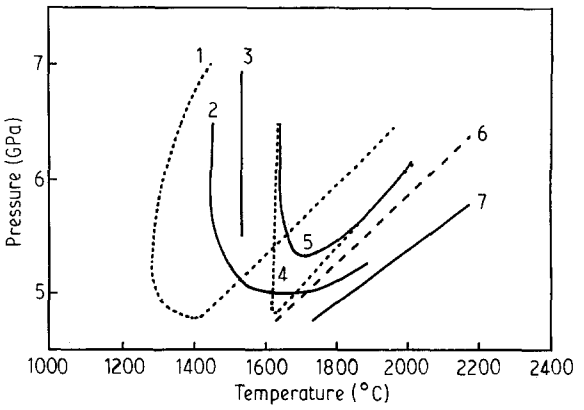

Figure 4 Cubic BN growth region in the system Li_3N–BN. Cubic BN exists in the region above each curve. (1) Vereshchagin *et al.* [20], (2) and (3) this work (see text), (4) De Vries and Fleischer [2], (5) Fukanaga *et al.*, [14], (6) Bundy–Wentorf hBN–cBN equilibrium line (see text), (7) close-to-true hBN–cBN equilibrium line after Rapoport (see text).

excluded, however, since in this case the boron liberated by the reaction

$$3Li + BN \rightarrow Li_3N + B \qquad (1)$$

would have been in sufficient concentration in the melt to colour the cBN crystals a dark brown or black, whereas all crystals were yellow or white.

At $T < 1350$ °C very small (approximately 1 µm) shapeless crystals grow with low yield. In this range we suggest the formation of cBN according to the following sequence of solid-state reactions

$$Li_3N + hBN \rightarrow Li_3BN_2 \qquad (2)$$

with

$$\Delta V/V = -10\%$$

$$Li_3BN_2 + hBN \rightarrow Li_3N + cBN + hBN \qquad (3)$$

with

$$\Delta V/V \simeq 0$$

$$Li_3N + cBN + hBN \rightarrow Li_3BN_2 + cBN \qquad (4)$$

with, for Reactions 3 and 4,

$$\Delta V/V = -9\%$$

where the volume changes have been calculated using the density of the low-pressure phase of Li_3BN_2 reported by Goubeau and Anselment [21] since the density of the high-pressure phase [22] is unknown. This approximation is not likely to modify $\Delta V/V$ greatly because pure crystallographic solid to solid transformations generally involve very small volume changes.

Reactions 3 and 4, considered as a whole, do not contradict the observation of De Vries and Fleisher [2] that the decomposition of Li_3BN_2 alone, in the field of stability of cBN, yields only hBN. Apart from kinetic considerations it can be noted that Reaction 3, or the decomposition of Li_3BN_2 alone by the Reaction

$$Li_3BN_2 \rightarrow Li_3N + cBN \quad (5)$$

relating to a volume change of approximately zero should be thermodynamically independent of pressure, whereas Reaction 2 and Reaction 3 followed by Reaction 4 lead to large volume contractions and are favoured by pressure through the $p\Delta V$ term in the Gibbs energy. The boron generated by Reaction 1 could serve as nuclei for the cBN crystals.

3.1.2.2. cBN crystals. The crystals formed in the Li_3N–BN system at $T > 1580\,°C$ were generally more perfect than with Ca_3N_2 or Mg_3N_2. They contained less inclusions and reached 0.25 mm; their shape was tetrahedral or octahedral, no platelets have been observed; their colour was a deeper yellow than with the other nitrides (see Fig. 5).

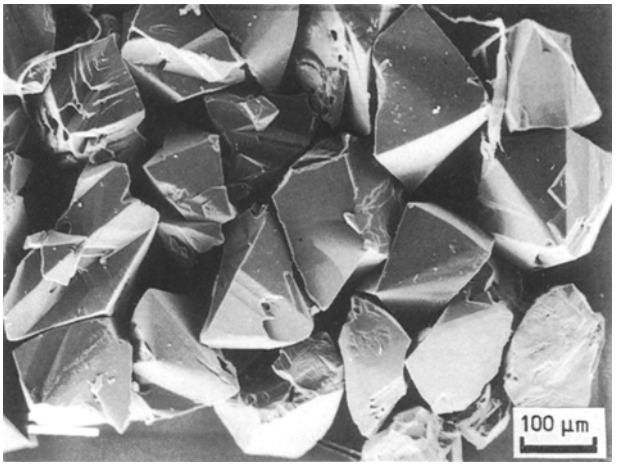

Figure 5 SEM micrograph of cubic BN crystals grown from the system Li_3N–BN.

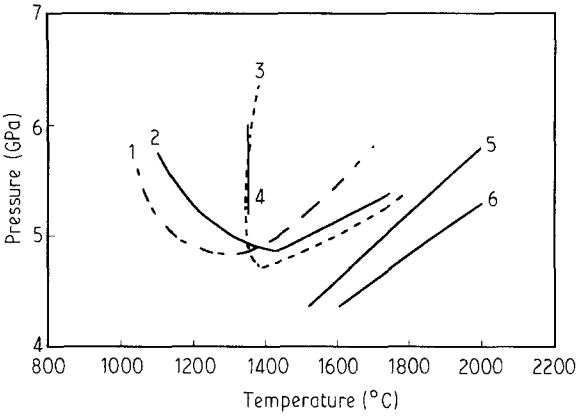

Figure 6 Cubic BN growth region in the system Ca_3N_2–BN. Cubic BN exists in the region above each curve: (1) De Vries and Fleischer [2], (2) this work, (3) Endo *et al.* [23] (from $Ca_3B_2N_4$ or Ca–BN), (4) this work, (5) Bundy–Wentorf hBN–cBN equilibrium line (see text), (6) close-to-true hBN–cBN equilibrium line after Rapoport (see text).

3.1.3. Ca_3N_2–BN

3.1.3.1. P–T diagram. As can be seen in Fig. 6 our results are in rough agreement with those of De Vries and Fleisher [2]. Differences in the method used for pressure calibration of the apparatus are probably at the origin of the discrepancies among high-temperature boundaries. The minimum synthesis pressure lies around 4.7 GPa at 1300 °–1400 °C. The high-temperature lines are closer to the Bundy–Wentorf than to the Rapoport hBN–cBN equilibrium line.

Also shown in Fig. 6 is the diagram reported by Endo *et al.* [23] for $Ca_3B_2N_4$–BN and Ca–BN. These authors have shown that the low-temperature limit of cBN formation in the two systems was closely related to the eutectic melting temperature in the system $Ca_3B_2N_4$–BN. Moreover they failed to synthesize cBN with Ca_3N_2 at 6 GPa between 1000 and 1300 °C and pointed out that a boundary related to an eutectic melting temperature should increase with pressure, contrary to the low-temperature data of De Vries and Fleisher [2]. Accordingly they assigned these data to hydrolysis of Ca_3N_2 by moisture. In our work, great care was taken to avoid pollution of Ca_3N_2 before and during the synthesis; therefore, we believe that the negative slope found both here and by De Vries and Fleisher [2] is intrinsic.

However, at temperature below about 1350 °C, the cBN yield was very small (a few percent) and may have been undetected by Endo *et al.* [23] who used X-rays to identify the phases. Moreover, in this region, the crystals had a polycrystalline blocky morphology similar to that observed with Mg_3N_2 (see further) at low temperature and characteristic of crystallization from a solid-to-solid reaction. Accordingly one can assume that the boundary of Endo *et al.* [23] and the temperature limit of 1350 °C observed by us relate to the eutectic melting of $Ca_3B_2N_4$–BN which divides the low-temperature region into two zones. At $T > 1350\,°C$ euhedral crystals grow from a liquid phase with an appreciable yield, whereas at $T < 1350\,°C$ anhedral crystals form from a solid-to-solid reaction with a very low yield. The distectic reaction involved would be the partial decomposition of $Ca_3B_2N_4$. The sequence of reactions in this scheme, similar to that reported above for Li_3N, is

$$Ca_3N_2 + 2hBN \rightarrow Ca_3B_2N_4 \quad (6)$$

with

$$\Delta V/V = -6\%$$

$$Ca_3B_2N_4 + 2hBN \rightarrow Ca_3N_2 + 2cBN + 2hBN \quad (7)$$

with

$$\Delta V/V = -4\%$$

$$Ca_3N_2 + 2cBN + 2hBN \rightarrow Ca_3B_2N_4 + 2cBN \quad (8)$$

with

$$\Delta V/V = -8\%$$

where the density of $Ca_3B_2N_4$ was taken from [21].

From a thermodynamical viewpoint Reactions 6–8 are favoured by pressure via the negative sign of the $p\Delta V$ term in the Gibbs energy. This would result in the lowering of the temperature threshold for formation of $Ca_3B_2N_4$ (Reaction 6), immediately followed by partial decomposition by Reaction 7. In this way the negative slope of the lower-temperature boundary on the diagram would be explained, together with the small yield observed in this region.

The preceding mechanism is not incompatible with the absence of decomposition of $Ca_3B_2N_4$ observed by Endo *et al.* [23] in a run where cBN was grown at 1540 °C and 5.6 GPa since the Gibbs energy of the system is more depressed by the formation of cBN in this P–T region by Reaction 7 followed by Reaction 8 than by decomposition of $Ca_3B_2N_4$ alone via Reaction 7.

3.1.3.2. cBN crystals. At temperatures higher than 1350 °C the cBN crystals are translucent yellow, often showing zones of lighter colour; their shape is that of truncated tetrahedra or pseudohexagonal platelets sometimes reaching 0.15 mm, but most often under 50 μm.

A dozen runs were made using preformed $Ca_3B_2N_4$ prepared at ambient pressure in the manner described by Endo *et al.* [23]. As these authors reported the compound to be much less hygroscopic than Ca_3N_2, the pellets were precompacted (by hand) in a glove box, as in the case of Li_3N and Mg_3N_2. The recovered cBN crystals were very small (10–20 μm) and the yield was lower than with Ca_3N_2 in contrast with the observations made by Endo *et al.* [23]; we do not understand the disagreement.

3.1.4. Mg_3N_2–BN

3.1.4.1. P–T diagram. Existing data on this system are shown in Fig. 7. Taking into account the fact that Elyutin *et al.* [24] used an apparatus of the toroid type, which differs from those of the belt or girdle type used by the other authors, the high temperature boundaries of the diagrams can be considered as roughly in agreement. They lie closer to the Bundy–Wentorf hBN–cBN equilibrium line than to that proposed by Rapoport. The minimum synthesis pressures range from 4.8 to 5.1 GPa at 1430–1500 °C.

The main differences between the diagrams appear in the lower temperature range. According to our

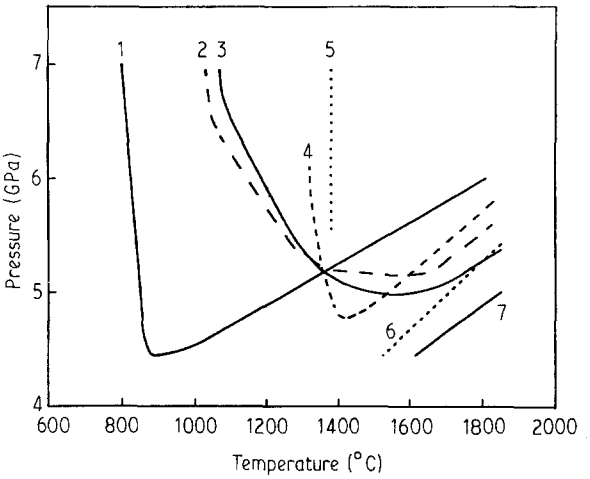

Figure 7 Cubic BN growth region in the system Mg_3N_2–BN. Cubic BN exists in the region above each curve: (1) Elyutin *et al.* [24], (2) Sato *et al.* [27], (3) this work, (4) De Vries and Fleischer [2], (5) this work (see text), (6) Bundy–Wentorf hBN–cBN equilibrium line (see text), (7) close-to-true hBN–cBN equilibrium line after Rapoport (see text).

observations this range can be divided into two regions corresponding to a different morphology of the cBN crystals and roughly limited by a vertical boundary at approximately 1380 °C. At $T > 1380$ °C crystals grow with facets suggesting growth from a liquid phase. At $T < 1380$ °C, nodules of very small crystals (approximately 1 μm) form. The threshold temperature coincides with the eutectic melting temperature of $Mg_3B_2N_4$ with excess BN reported by Hohlfeld [25] from differential thermal analysis (DTA) measurements at 6.5 GPa. Our finding is then in agreement with the statement that at $T > 1380$ °C, cBN grows from liquid $Mg_3B_2N_4$ saturated with BN.

In the range 1230–1430 °C peculiar features of the conversion kinetics, more precisely a maximum of hBN–cBN conversion rate at 1230–1330 °C followed by a minimum at 1330–1380 °C, have been observed by Elyutin *et al.* [24] and confirmed by Lorenz *et al.* [26]. Although the temperatures of the extrema are slightly different in the two studies and a better resolution is obtained by Lorenz *et al.*, the peculiarities should refer to the same phenomenon.

In the present work where the kinetics of the hBN–cBN transformation were not systematically investigated, the preceding peculiarities were not observed for some of the following possible reasons: the cell arrangement was different (alternate disks of hBN and Mg_3N_2 instead of mixed powders), or the temperature gradients in the sample and the temperature interval between different runs were too large.

The low temperature boundary reported by De Vries and Fleisher [2] which is close to 1330° C at 6 GPa probably relates to the lowest temperature limit of the high hBN–cBN conversion range, 1330–1380 °C, observed by Lorenz *et al.* [26]. The peculiarities in the conversion kinetics mentioned above are interpreted by the quoted authors on the basis of solid-to-solid reactions producing cBN. For Elyutin *et al.* [24], the reaction involves decomposition of $Mg_3B_2N_4$ which

has two modifications at HP–HT with different stability. For Hohlfeld [25], $Mg_3B_2N_4$ is formed in a two-step mechanism via Mg_3BN_3 before it decomposes. In the present work, although a few X-ray diagrams of the reaction products were made by the quenching process, these diagrams do not allow one of the two interpretations to be chosen over the other.

The low temperature boundaries observed by Sato *et al.* [27] and in the present work suggest a solid-state mechanism liberating cBN in its stability field where the driving force increases with pressure, because their slope is negative. A reaction or a sequence of reactions involving a net volume contraction are thus required. For instance one may think of reactions similar to the sequences given above in the case of Li_3BN_2 and $Ca_3B_2N_4$. However the density of $Mg_3B_2N_4$ has not been determined, and the volume changes cannot be calculated.

3.1.4.2. cBN crystals. The cBN crystals are most often agglomerated even when exhibiting translucent parts and facets. Exceptionally they are isolated tetrahedra, generally opaque, and under 50 μm. Their colour varies from orange to white. In agreement with previous findings MgO was almost always found on the crystals despite the low oxygen content of the starting BN. The crystals grown at $T > 1380\,^{\circ}C$ showed acute corners and sharp edges however.

3.1.5. General comments on the Mg–BN and MxNy–BN systems

The present work reveals the existence of two regions in the P–T cBN-formation zone of the Li_3N–, Ca_3N_2–, and Mg_3N_2–BN systems. The high-temperature region limited by the eutectic temperature in the corresponding systems and the equilibrium hBN–cBN line yields faceted crystals grown from a liquid phase. The low-temperature region limited by the preceding eutectic temperature and a lower threshold generally decreasing with increasing pressure (for Mg_3N_2 and Ca_3N_2) yields very small shapeless crystals, often agglomerated, resulting from precipitation of cBN in solid-state reactions. Due to varying experimental conditions (arrangement of the cell, environment, kinetic parameters) one or the other of the two-low temperature boundaries has been observed by the investigators leading to apparent discrepancies in the diagrams.

Solid-state reactions producing cBN are proposed on the basis of thermodynamic considerations for the three nitrides. Besides, the presence of a few percent of Li in our starting Li_3N, and perhaps a slight decomposition of it in our experiments, leads to a 80 °C decrease in the minimum temperature for a liquid-phase appearance.

For the Mg–BN system our data confirm previous data showing an effect of the O_2 content of the starting BN on the cBN formation diagram.

To summarize our results for the cBN crystals, an important yield was observed with the three nitrides in the high-temperature zone, the quality and size of the single crystals increases in the sequence of initiators Mg_3N_2, Ca_3N_2, Li_3N; with Mg as initiator the yield was low and most crystals were of medium quality.

3.2. MxNy–M′–BN systems

3.2.1. Results

The initiator consisted of pellets of MxNy and M′ powders in given proportions, intimately mixed and compacted in a glove box. The same cell was used as for the pure nitrides (see Fig. 1). As it was first suspected that the effect of M′ addition on the cBN growth would roughly reflect the degree of the reduction of the nitride MxNy, experiments were made with increasing proportions of M′ up to at least the value corresponding to an hypothetic total reduction calculated from reactions of the type

$$Ca_3N_2 + 2Al \rightarrow 3Ca + 2AlN \qquad (9)$$

which for M′ = Al, B, Si, and Ti yields the nitrides AlN, BN, Si_3N_4 and TiN. Exceptionally percentage of the M′ was not increased up to the calculated value in the case of Ca_3N_2 + Ti because the change in cBN crystals was completed at a lower percentage of M′; and in the case of Mg_3N_2 + Al because the crystals were of medium quality.

The influence of M′ on the P–T diagram for cBN formation appears in the minimum synthesis pressures at 1700 °C, $(P_{min})_{1700\,^{\circ}C}$, which are given in Table III for two values of M′ %: the approximate minimum value (indicated by an asterisk in Table III) for appearance of crystals of improved morphology and the maximum value investigated.

Except for Ca_3N_2 + Ti at low Ti %, the minimum pressures P_{min} at 1700 °C are seen to increase with increasing M′ content from the pure nitride values.

TABLE III Minimum CBN synthesis pressures at 1700 °C in (MxNy + M′)–BN systems

MxNy	M′	$\frac{m(M')}{m(MxNy)}$ (%)	P_{min} (GPa) at 1700 °C
Li_3N	–	–	5.0
Li_3N	Al	35*	5.2
		100	5.9
Li_3N	B	10*	5.2
		30	5.9
Li_3N	Si	20*	5.6
		60	6.0
Ca_3N_2	–	–	5.2
Ca_3N_2	Al	10*	5.2
		100	5.7
Ca_3N_2	B	5*	5.3
		30	5.5
Ca_3N_2	Ti	15*	5.0
		35	5.3
Ca_3N_2	Si	10*	5.5
		30	5.9
Mg_3N_2	–	–	5.0
Mg_3N_2	Al	25*	5.4
Mg_3N_2	B	10*	5.0
		25	5.2

*Minimum value for appearance of crystals of improved morphology

Correspondingly the cBN yield at a given pressure, at 1700 °C, was generally found to decrease with increasing M′%. However, this yield remained substantially higher than that obtained with pure M metals as initiators, a factor of five, approximately, being observed, for instance, in the case of Ca_3N_2 + 2Al and Mg_3N_2 + 2Al mixtures compared to Ca and Mg.

As the proportion of M′ increased to the minimum value for appearance of crystals of improved morphology, the originally orange or yellow crystals obtained for pure nitrides turned to a paler yellow or even to colourless crystals. This effect was particularly marked with elements Ti, B and Al. At higher M′-content dark zones appeared in the crystals (Fig. 8) and entirely dark crystals also appeared. Finally, at the highest M′ content all crystals were of the dark type. If the yellow colour of cBN is due to oxygen as has been suggested [28], this could be because it is gettered by M′ in the low-doped systems before the concentration of boron in the flux and crystal became sufficient to give the black tint. The dark crystals had a more perfect and more compact morphology than the yellow crystals, as can be seen in Fig. 9 and their maximum size was 0.6 mm instead of 0.25 mm. The crystals obtained with the Mg_3N_2–M′ systems showed little improvement compared to the pure nitride systems, however.

For each system an M′ concentration could be defined corresponding to the lowest M′% for which the majority of crystals belong to the dark type. This is compared to the concentration calculated from Reaction 9 in Table IV. The corresponding minimum synthesis pressures at 1700 °C were found to increase in the M′ sequence: Al, B, Ti, Si.

3.2.2. Discussion

Although the composition of the flux and of the other phases present during the synthesis was not studied in our work, the preceding results call for several remarks. Firstly, the increase in the minimum synthesis pressure at 1700 °C with increasing M′% in all the investigated systems (see Table III) probably relates to an increase of the minimum temperature of appearance of a liquid phase. Secondly, Table IV shows that there is a rough correlation between the composition of initiator corresponding to the change from the orange type of crystal to the dark and full reduction of MxNy by Reaction 9. This gives support to the assumption that the synthesis involves Reaction 9, at least in those cases where no ternary nitride (other than the boronitride) is formed since, then, when the stoichiometry of Reaction 9 is realized, the starting (MxNy + M′)–BN systems transform to the M–BN systems (with additional nitrides) which are known to produce dark crystals. No ternary nitride is known at ambient pressure for the following MM′ couples: Ca–Al, Ca–Ti, Li–Si: In the case of Li–B, Ca–B and Mg–B couples, the ternary nitride is the boronitride itself which is the solvent. In those systems, a larger yield is observed with doped nitrides than pure metals; this is probably related to the greater reactivity of the activated M species produced by Reaction 9 relative to the metals themselves.

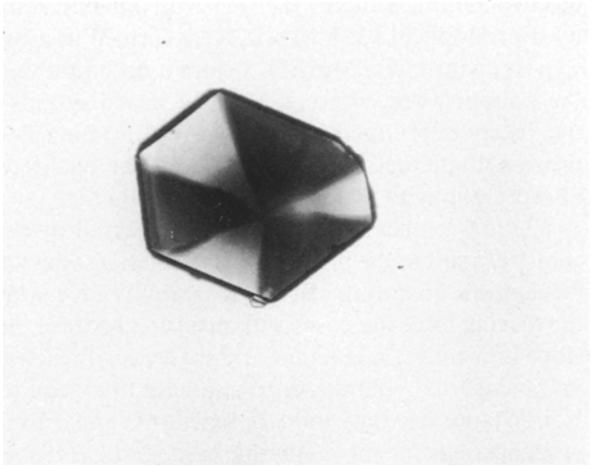

Figure 8 Cubic BN crystal grown from the system (Ca_3N_2 + 0.1 Al)–BN showing sectorial dark zones.

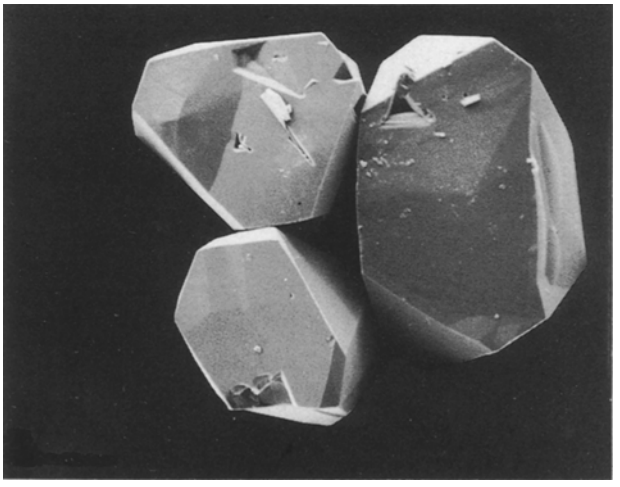

Figure 9 SEM micrograph of typical cubic BN crystals grown from systems (MxNy + M′)–BN with M′% close to the value calculated from Reaction 9 (see Table IV).

TABLE IV Concentration of M′ relative to MxNy corresponding to Reaction 9 (calculated) and to the change of cBN crystal type (observed) in (MxNy + M′)–BN systems.

MxNy	M′	M′ (mass %)		
		Explored range	Calculated	Observed
Li_3N	Al	0–100	77	70
"	B	0–40	31	30
"	Si	0–60	60	50
Ca_3N_2	Al	0–100	36	30
"	B	0–30	15	15
"	Ti	0–50	65	50
"	Si	0–30	30	30
Mg_3N_2	Al	0–30	54	> 30
"	B	0–20	20	20

Ternary nitrides (other than the boronitrides) are known for the following MM′ couples: Ca–Si [29], Mg–Al [30], and Li–Al [31]. In this case the physicochemical processes are presumably more complex and

the correlation observed between the M′% values in Table IV is probably fortuitous. Two possibilities can be imagined, depending on the stability of the ternary nitride. If it is very stable, as is the case for the Ca–Si and Mg–Al nitrides, its formation will consume the MxNy nitride without producing cBN. This should result in an increase of the minimum P–T for synthesis and in a decrease of the yield compared to the other systems. Alternatively, if the ternary nitride is unstable at high pressure and temperature, particularly in the presence of BN, it may dissolve in the boronitride or play the role of solvent. An example of this is given by Li_3AlN_2; this compound is stable up to about 1100 °C at ambient pressure whereas Li_3BN_2 melts at 880 °C. However, Al has been found to form an AlN–BN solid solution in the peripheric layers of cBN crystals grown from a mixture of AlN + Li_3N as initiator [32]. This means that Li_3AlN_2 (or AlN) dissolves in the flux (Li_3BN_2) without hindering the crystallization of cBN and explains the moderate increase in P_{min}.

The increase in the minimum synthesis pressure at 1700 °C in the sequence M′ = Al, B, Ti, Si, observed in this work may however, be related to an increase in the minimum temperature of the appearance of a liquid phase, and related to the different degree of solubility of M′ in the flux and in the cBN crystals. A charge effect may explain that the tetravalent metals Si and Ti require higher pressures than the trivalent metals (Al, B) more easily captured by the cBN crystals. The inhibiting effect of Si on the cBN crystallization has already been observed by Yoshihara *et al.* [33] in the B–N–Si system.

Finally, there are particular M′ nitrides formed during Reaction 9 which are known to initiate the crystallization of cBN; this is the case of AlN [34] and Si_3N_4 [35] which yield colourless crystals of very small size (1–10 μm) through unknown solid-state reactions. The following facts support our opinion that these processes do not play a role in the systems reported here. Firstly, the fully reducing conditions which are said in [32] to be necessary for the synthesis with AlN, at least in the P–T range explored in our work (<6 GPa), are not realized in our experiments; secondly, at the P–T conditions reported for Si_3N_4 in [35] (i.e. 6GPa–1800 °C) a liquid phase is formed in our systems. Thirdly, the cBN crystals are completely different in size and colour from those obtained in the present work.

4. Conclusion

The P–T formation diagrams of cBN using Li_3N, Mg_3N_2 and Ca_3N_2 as initiators have been redetermined. Compared to previous data, the minimum synthesis pressures and the high temperature boundaries show some discrepancies which are probably due to uncertainties in the pressure and temperature measurements. At lower temperatures the boundary is not determined by an eutectic temperature but by the kinetics of formation of cBN in the solid state due to the decomposition *in situ* of the boronitrides. The crystals are then very small and anhedral. The temperature above which euhedral crystals are formed defines roughly the eutectic between BN and the boronitrides. This behaviour was observed by some authors (and not by others) perhaps because of different environments of the samples.

It has been shown that doping of the above mentioned nitrides MxNy by M′ = Al, B, Ti, Si induces a change in the morphology and colour of cBN crystals at about the stoichiometric proportion corresponding to full reduction of the nitride. The new crystals are dark instead of orange and more compact and perfect than the orange ones. Doping increases the minimum synthesis pressure (at 1700 °C) differently for the four M′ elements. At given P–T conditions the yield is substantially higher than when pure M metals are used.

Acknowledgements

We wish to express our gratitude to Ch. Bogicevic and F. Clerc for the chemical treatments of the samples and C. Bahezre for the SEM micrographs.

References

1. R. H. WENTORF, *J. Chem. Phys.* **34** (1961) 809.
2. R. C. DE VRIES, J. F. FLEISHER, *J. Cryst. Growth* **13/14** (1972) 88.
3. T. SATO, T. ENDO, S. KASHIMA, O. FUKUNAGA, M. IWATA, *J. Mater. Sci.* **18** (1983) 3054.
4. T. ENDO, O. FUKUNAGA, M. IWATA, *J. Mater. Sci.* **14** (1979) 1676.
5. H. M. STRONG, R. E. TUFT, G. E. Report N°74 CR D118 (Corporate Research and Development Distribution, Schenectady, N.Y., 1974).
6. G. BOCQUILLON, C. LORIERS-SUSSE, J. LORIERS, *J. Mater. Sci. Lett* **4** (1985) 141.
7. I. C. GETTING, G. C. KENNEDY, *J. Appl. Phys.* **41** (1970) 4552.
8. J. THOMAS Jr, N. E. WESTON, T. E. O'CONNER, *J. Amer. Chem. Soc.* **84** (1963) 4619.
9. F. B. BUNDY, R. H. WENTORF Jr, *J. Chem. Phys.* 38 (1963) 1144.
10. E. TANI, T. SOMA, A. SAWAOKA, S. SAITO, *Jap. J. Appl. Phys.* **14** (1975) 1605.
11. E. RAPOPORT, *Ann. Chim. Fr.* **10** (1985) 607.
12. F. R. CORRIGAN, F. P. BUNDY, *J. Chem. Phys.* **63** (1975) 3812.
13. T. ENDO, O. FUKUNAGA, M. IWATA, *J. Mater. Sci.* **14** (1979) 1375.
14. O. FUKUNAGA, T. SATO, M. IWATA, H. HIRAOKA, Proceedings of the 4th International Conference on High Pressure, Kyoto, in the Review of Physical Chemistry of Japan (Kawakita, Kyoto, 1975) p. 454.
15. M. M. BINDAL, S. K. SINGHAL, B. P. SINGH, R. K. NAYAR, R. CHOPRA, A. DHAR, *J. Cryst. Growth* **112** (1991) p. 386.
16. K. KUDAKA, H. KONNO, T. MATOBA, *Kogyo Kagaku Zasshi* (J. Chem. Soc. Japan, Ind. Chem. Section) **69** (1966) 365.
17. M. USHIO, H. SAITO, S. NAGANO, *ibid.* **74** (1971) 598.
18. M. M. BINDAL, B. P. SINGH, S. K. SINGHAL, R. K. NAYAR, R. CHOPRA, A. DHAR, *J. Mater. Sci.* **26** (1991) 196.
19. N. E. FILONENKO, V. I. IRANOV, L. I. FEL'DGUN, M. I. SOKHOR, L. F. VERESHCHAGIN, *Dokl. Akad. Nauk. SSSR* **175** (1967) 1266.
20. L. F. VERESCHAGIN, I. S. GLADKAYA, G. A. DUBITSKII, V. N. SLESAREV, *Izv. Akad. Nauk. SSSR, Neorg. Mater.* **15** (1979) p. 256.
21. Von. J. GOUBEAU, W. ANSELMENT, *Zeit. f. anorg. allg. Chemie* **310** (1961) p. 248.

22. R. C. DE VRIES, J. F. FLEISHER, *Mat. Res. Bull.* **4** (1969) 433.
23. T. ENDO, O. FUKUNAGA, M. IWATA, *J. Mater. Sci* **16** (1981) 2227.
24. V. P. ELYUTIN, N. I. POLUSHIN, K. P. BURDINA, V. P. POLYAKOV, Ya. A. KALASHNIKOV, K. N. SEMENENKO, Yu. A. PAVLOV, *Dokl. Akad. Nauk. SSSR*, **259** (1) (1981) 112.
25. C. HOHLFELD, *J. Mater. Sci. Lett.* **8** (1989) 1082.
26. H. LORENZ, B. LORENZ, U. KUHNE, C. HOHLFELD, *J. Mater. Sci.* **23** (1988) 3254.
27. T. SATO, H. HIRAOKA, T. ENDO, O. FUKUNAGA, M. IWATA, *J. Mater. Sci.* **16** (1981) 1829.
28. R. C. DE VRIES, General Electric Report N°72 CR D178, (1972).
29. Y. LAURENT, *Rev. Chim. Miner.* **5** (1968) 1019.
30. J. W. DIETZ, US Patent 3531245, (1970).
31. R. JUZA, K. LANGER, K. Von BENDA, *Angew. Chem. International Edit.* **7** 5 (1968) 360.
32. B. G. ALESHIN, A. A. SMEKHNOV, A. N. SOKOLOV, A. A. SHULZHENKO, *Dokl. Akad. Nauk. Ukr. SSR* **12** (1984) 71.
33. H. YOSHIHARA, A. ONODERA, K. SUITO, H. NAKAE, Y. MATSUNAMI, T. HIRAI, *J. Mater. Sci.* **25** (1990) 4595.
34. S. HIRANO, T. YAMAGUCHI, S. NAKA, *J. Amer. Ceram. Soc.* **64** (12) (1982) 734.
35. Kabushiki Kaisha Komatsu Seisakusho, Brevet Francais N°74.08714, (1974).

Received 8 April
and accepted 29 October 1992